

Supporting Information for

Development of Sialic Acid-coated Nanoparticles for Targeting Cancer and Efficient Evasion of the Immune System

Young-Hwa Kim^{1#}, Kyung Hyun Min^{1#}, Zhantong Wang¹, Jihoon Kim¹, Orit Jacobson¹, Peng Huang², Guizhi Zhu¹, Yijing Liu¹, Bryant Yung¹, Gang Niu^{1*}, and Xiaoyuan Chen^{1*}

¹Laboratory of Molecular Imaging and Nanomedicine, National Institute of Biomedical Imaging and Bioengineering, National Institutes of Health, Bethesda, Maryland 20892, United States

²Guangdong Key Laboratory for Biomedical Measurements and Ultrasound Imaging, School of Biomedical Engineering, Shenzhen University, Shenzhen 518060, P. R. China

These authors contributed equally to this work.

Corresponding Author: Gang.Niu@nih.gov; shawn.chen@nih.gov

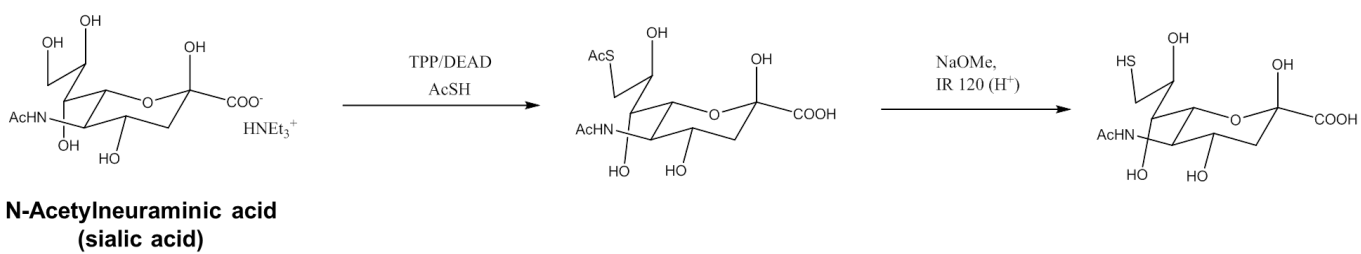


Figure S1. Synthesis of thiolated sialic acid

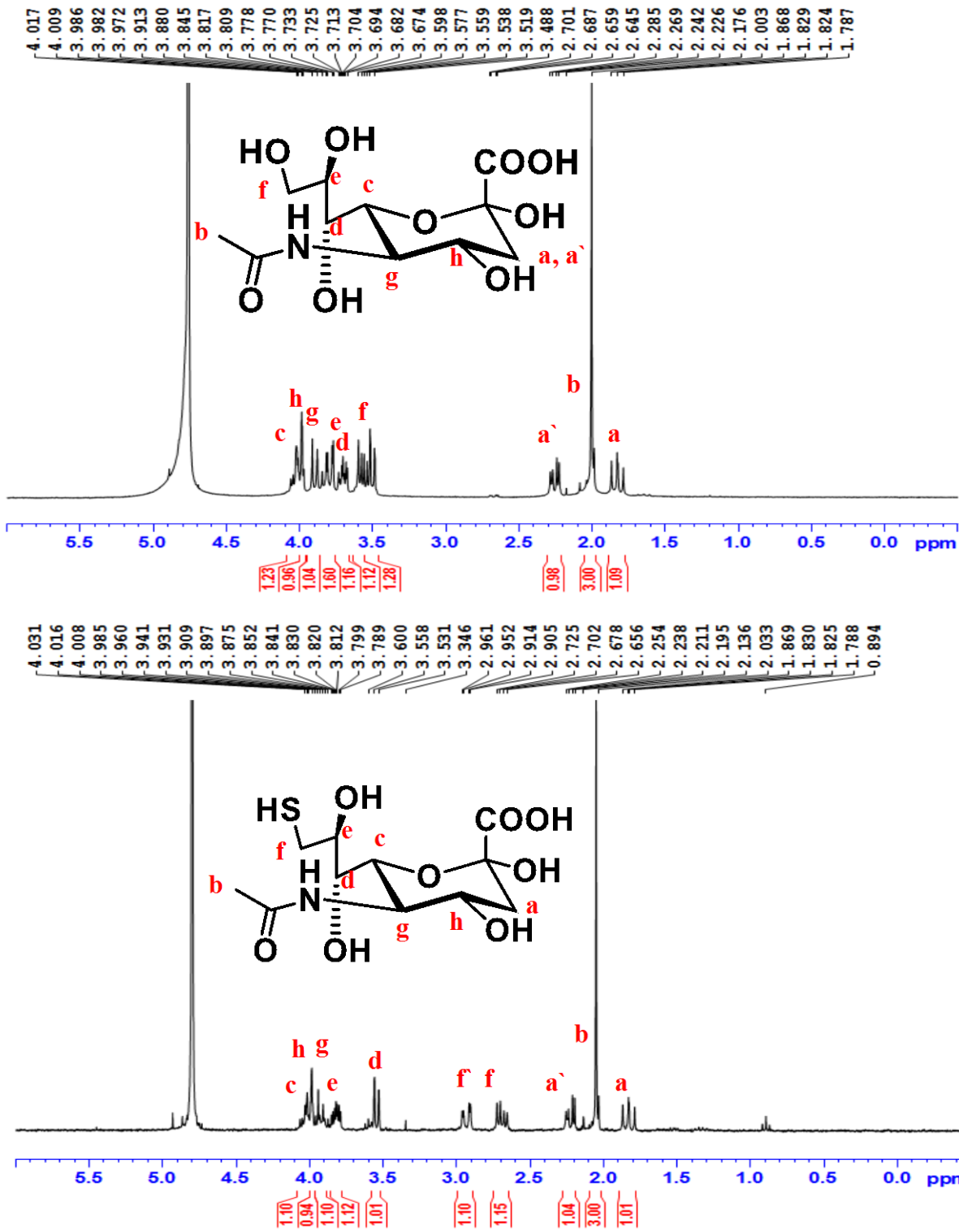
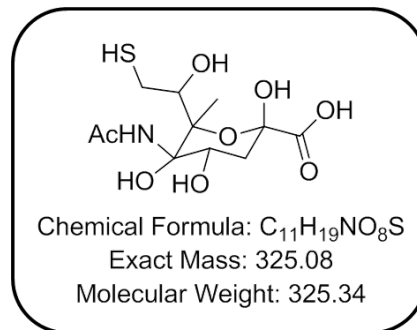
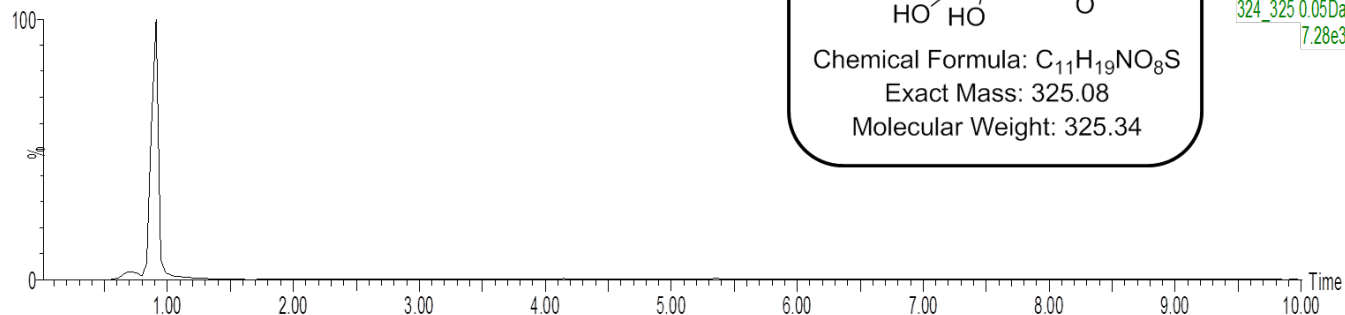


Figure S2. Confirmation of thiolated sialic acid using $^1\text{H-NMR}$

SA-SH

0

Ying-11-13-2015-02



13-Nov-2015

16:15:25

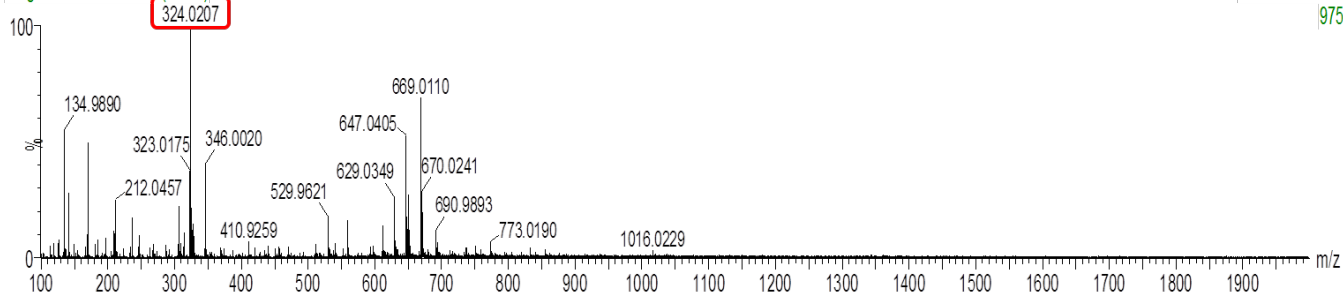
1: TOF MS ES-

324_325 0.05Da

7.28e3

SA-SH

Ying-11-13-2015-02 25 (0.911)



13-Nov-2015

16:15:25

1: TOF MS ES-

975

Figure S3. Confirmation of thiolated sialic acid using LCMS

Table S1. Hydrodynamic diameter (D_H) and zeta (ζ)-potential of the AuNPs. This table shows the zeta potential values, particle size, and PDI for various different kinds of AuNPs after modifying PEG and silaic acid onto the surface.

Sample	Zeta Potential (mV)	Z-Average(nm)	PDI
Unmodified AuNPs	-52.54 ± 2.30	25.56 ± 0.9	0.29 ± 0.09
Sialic Acid/mPEG AuNPs	-8.01 ± 1.15	39.40 ± 0.33	0.35 ± 0.04
COOH-PEG AuNPs	-36.33 ± 4.98	47.62 ± 0.73	0.31 ± 0.06
mPEG AuNPs	-0.12 ± 0.08	50.66 ± 0.9	0.28 ± 0.04
NH ₂ -PEG AuNPs	21.12 ± 2.03	52.22 ± 0.9	0.31 ± 0.06

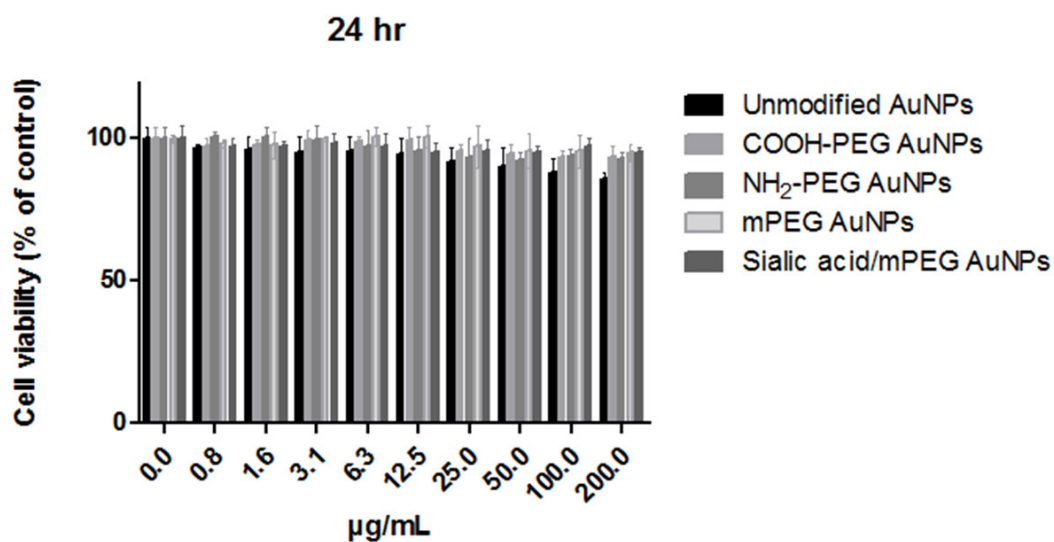
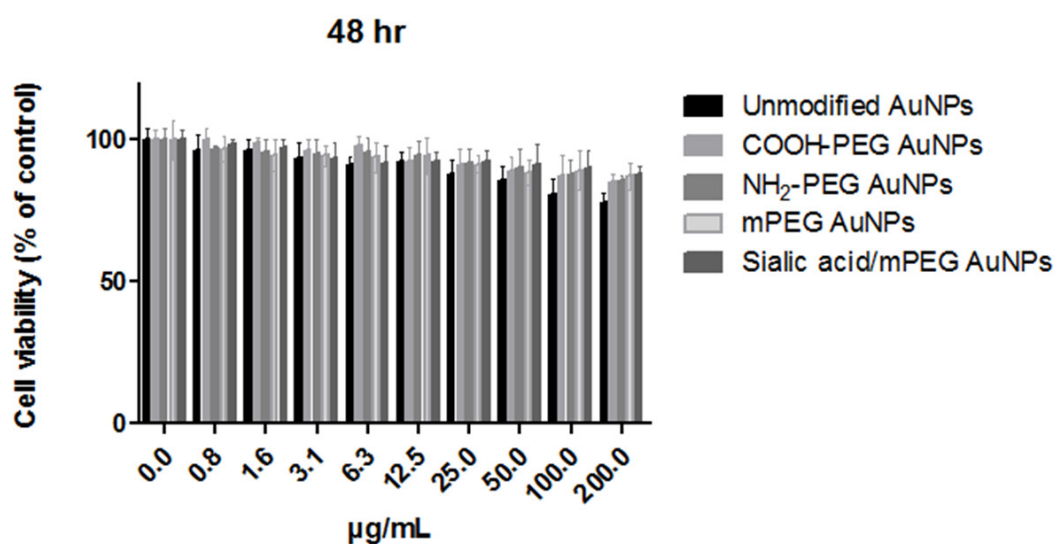
a**b**

Figure S4. Cell viability assay. RAW264.7 cells were treated with different amounts of AuNPs and incubated for 24 h (a) and 48 h (b), respectively. The results are presented as percentage absorbance relative to control cells incubated in a probe-free medium. Data represent mean \pm s.d of three independent experiments.

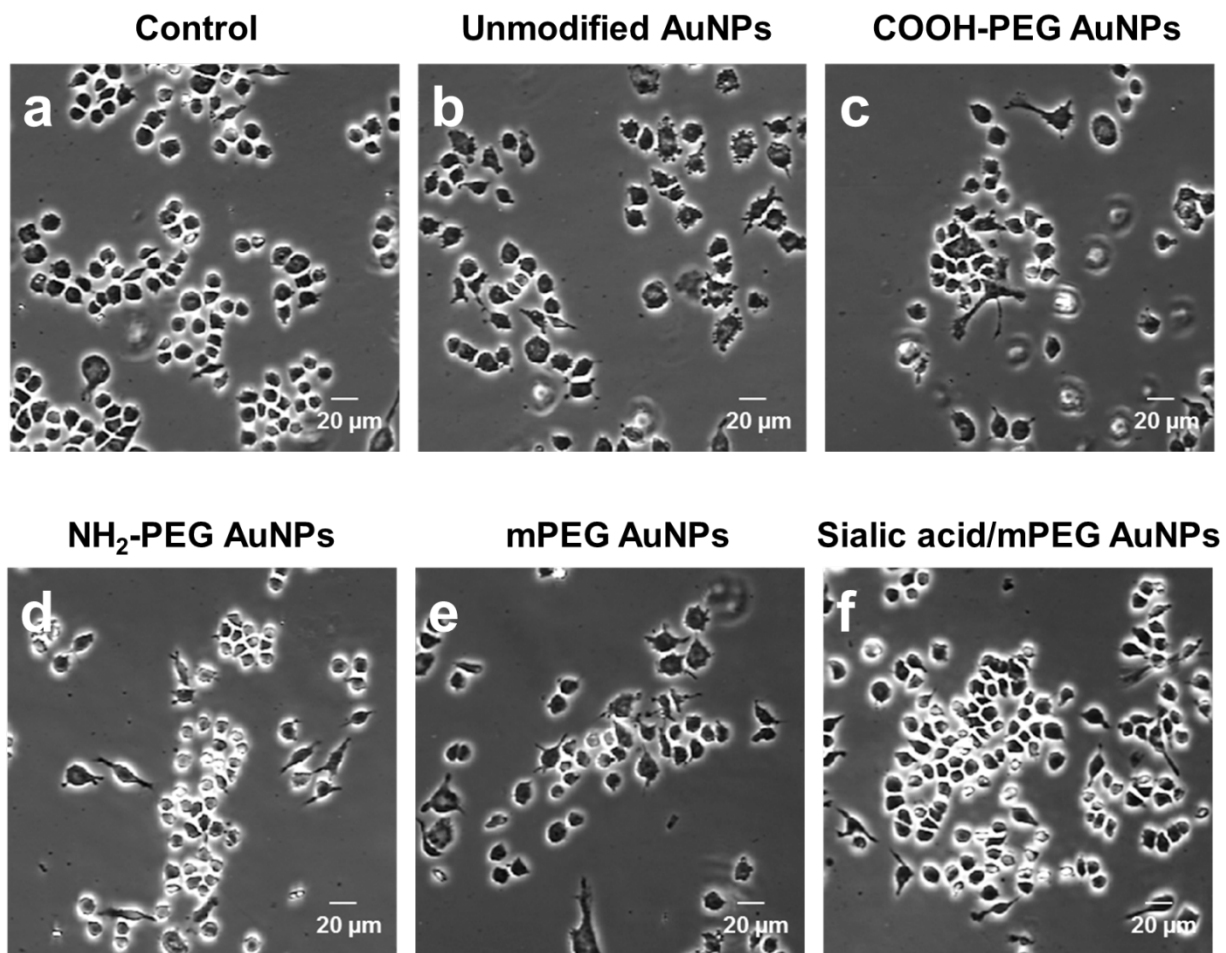


Figure S5. Morphological comparison among different AuNPs treated RAW264.7 cells.

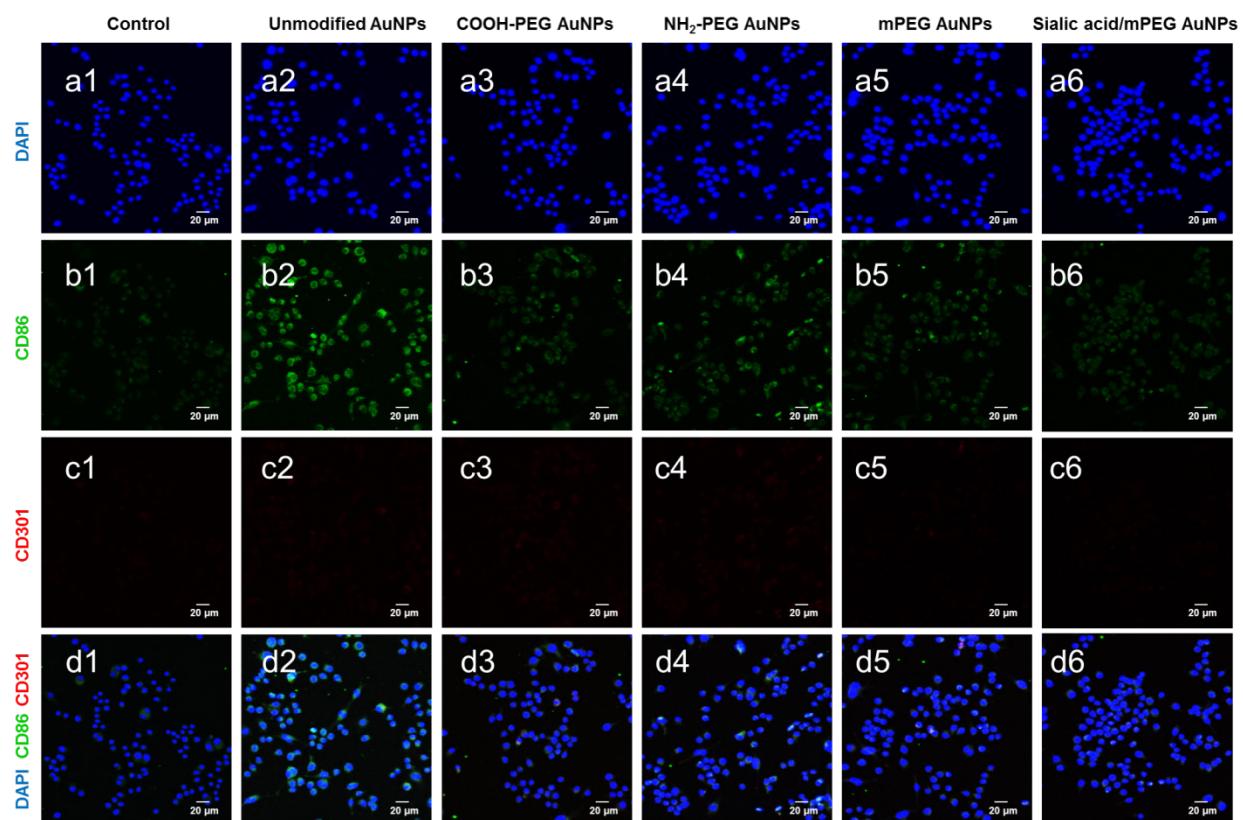


Figure S6. Representative confocal microscopy images of macrophage markers (CD86, CD301) in RAW264.7 cells after AuNPs treatment. Macrophage markers, CD86 and CD301, were stained in RAW264.7 cells after AuNPs (15 $\mu\text{g}/\text{mL}$) treatment for 24 hr, respectively. (a) Nuclei are stained with DAPI (blue). (b) Classical activated macrophage surface marker, CD86 is observed green fluorescence signals in the cell membrane surface. (c) Alternatively activated macrophage surface marker, CD301 is observed red fluorescence signals in the cell membrane surface. (d) It shows merged image of DAPI, CD86, and CD301. scale bar = 20 μm

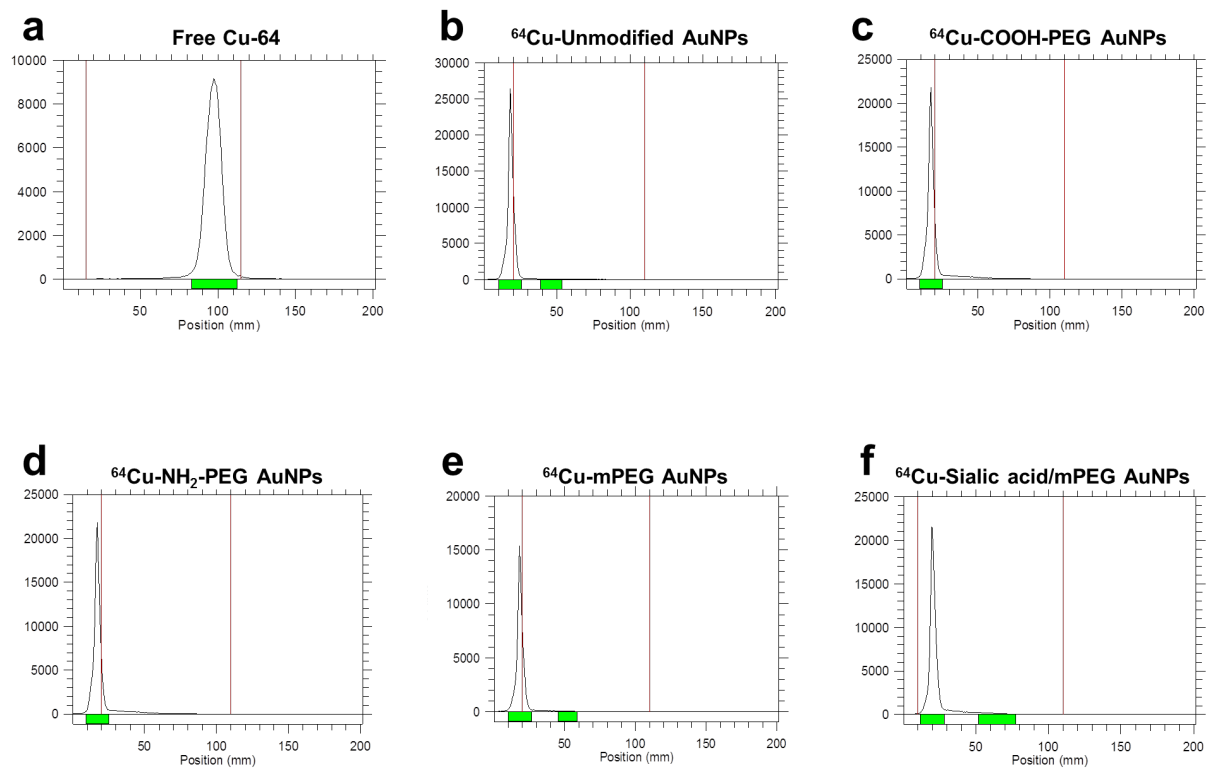


Figure S7. ITLC plate analyses of free Cu-64 and ^{64}Cu -AuNPs.

Table S2. Area under the curve (AUC) of major organs

Sample	Heart	Spleen	Liver	Tumor
Unmodified AuNPs	9.99	41.72	90.54	6.03
Sialic Acid/mPEG AuNPs	56.14	21.16	51.57	14.28
COOH-PEG AuNPs	34.62	32.78	51.49	7.77
mPEG AuNPs	40.76	32.63	54.21	9.03
NH ₂ -PEG AuNPs	44.24	32.18	60.02	10.03

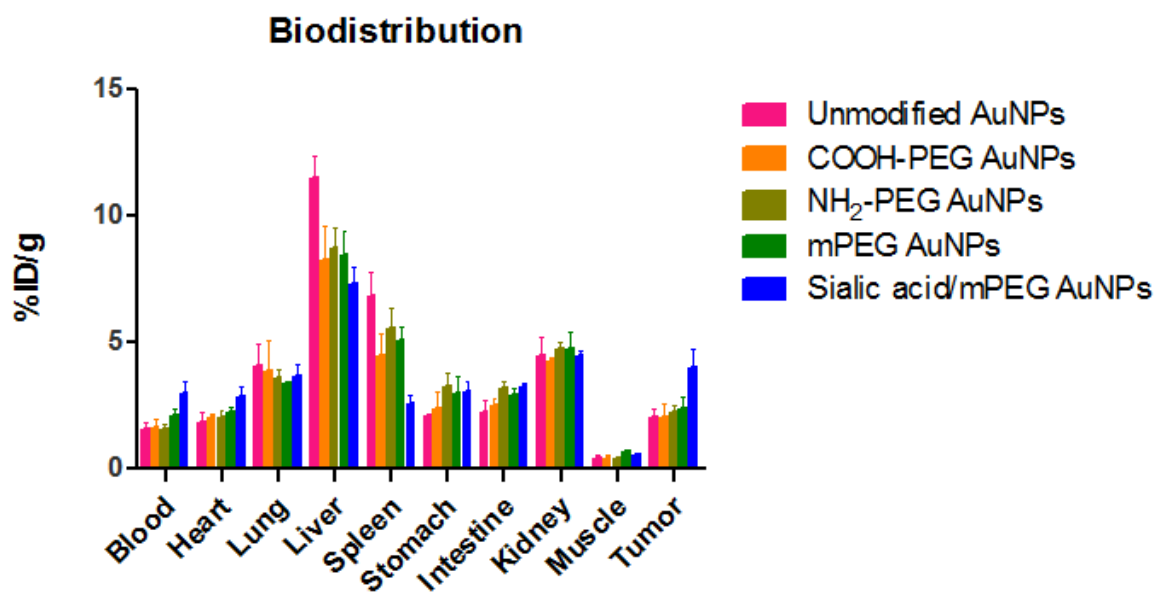


Figure S8. Biodistribution of ⁶⁴Cu-unmodified AuNPs, ⁶⁴Cu-COOH-PEG-AuNPs, ⁶⁴Cu-NH₂-PEG-AuNPs, ⁶⁴Cu-mPEG-AuNPs, and ⁶⁴Cu-sialic acid/mPEG-AuNPs, 1.85 MBq (50 μCi) in the blood and major organs at 50 h time point after i.v injection. (n = 4/group)

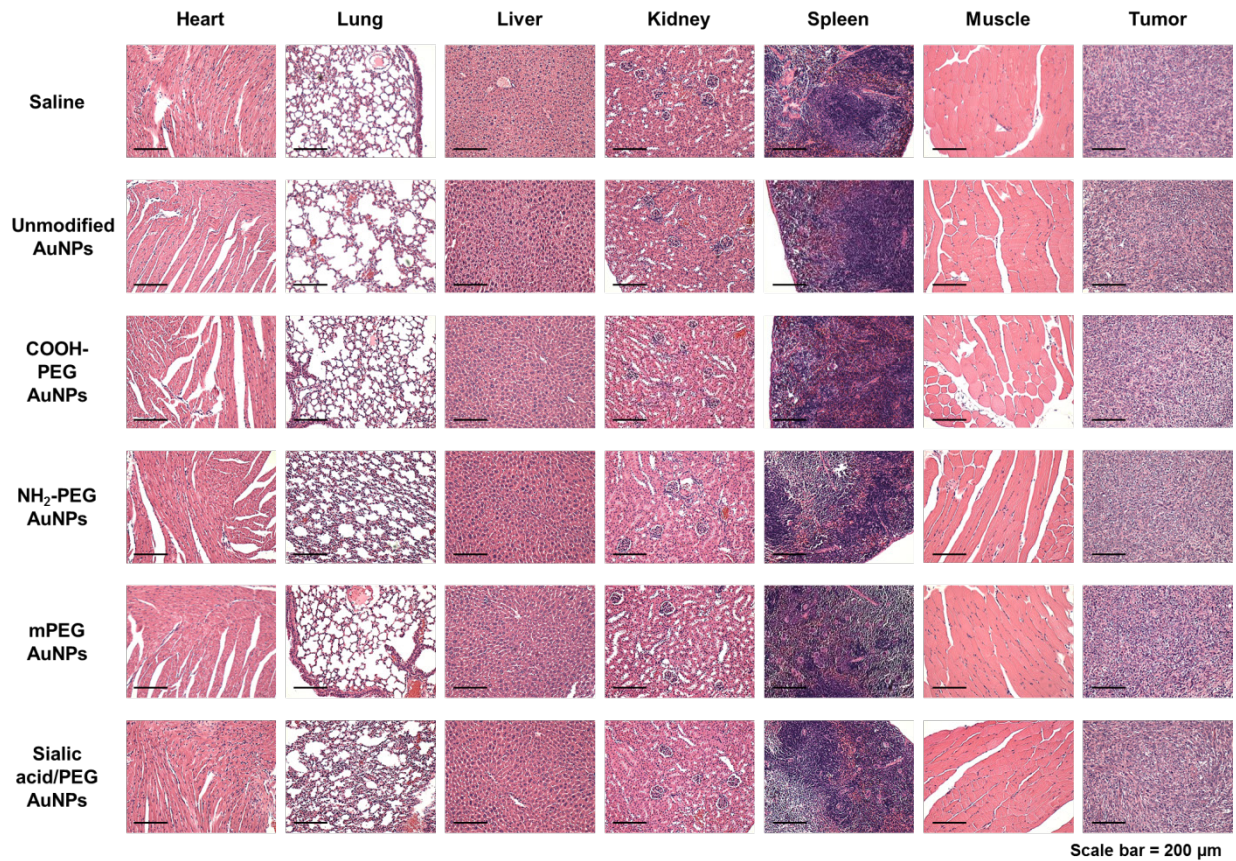


Figure S9. H&E staining of major organs after i.v injection of different AuNPs